Design and Fabrication of a Two Degree-of-Freedom Hopping Robot with Parallel Architecture using Linear Lorentz-force Actuators

by

Robert A. Hummel

Submitted to the Department of Mechanical Engineering
in Partial Fulfillment of the Requirements for the Degree of
Bachelor of Science in Mechanical Engineering

at the

MASSACHUSETTS INSTITUTE OF TECHNOLOGY

June 2009

Signature of Author.....
Department of Mechanical Engineering
May 8, 2009

Certified by.....
Ian W Hunter, PhD
Hatsopoulos Professor of Mechanical Engineering
Director, Laboratory for Bioinstrumentation
Thesis Supervisor

Accepted by.....
Professor J. Lienhard V
Collins Professor of Mechanical Engineering
Chairman, Undergraduate Thesis Committee

Design and Fabrication of a Two Degree-of-Freedom Hopping Robot with Parallel Architecture using Linear Lorentz-force Actuators

by

Robert A. Hummel

Submitted to the Department of Mechanical Engineering
on May 8, 2009 in partial fulfillment of the requirements for the
Degree of Bachelor of Science in Mechanical Engineering

ABSTRACT

This thesis presents the design and fabrication of a 2-DOF robotic leg using linear Lorentz-force actuators arranged in a parallel configuration. The decision to use linear actuators, a parallel architecture, and Lorentz-force motors was made because of distinct differences between these designs and the alternatives, notably, their lower weight, better resolution, and high bandwidth. We have shown that a robot of this construction can jump at least three times as high as the stroke length of its actuators, recording a maximum jump height of 48 mm using a stroke of 15 mm. This finding supports the feasibility of a larger robot based on this design.

Thesis Supervisor: Ian W. Hunter
Title: Hatsopoulos Professor of Mechanical Engineering

Contents

List of Figures

1.0 Introduction

The goal of this thesis is to design and build a two degree-of-freedom jumping robot with parallel architecture using linear Lorentz-force actuators [1]. Each of these characteristics offers distinct advantages over the alternatives. No other robot has combined these characteristics in a single machine, nor has jumping or walking robot used Lorentz-force linear actuators for movement. This thesis will attempt to support the feasibility of using Lorentz-force linear actuators in such a manner.

2.0 Background

2.1 Jumping Robots

Jumping robots have been studied extensively for many years. Prof. Mark Raibert of MIT used jumping robots as a means of studying dynamic balancing in inherently unstable systems [2]. Figure 1 shows Prof. Raibert's 3D One-legged Hopper, developed at the MIT Leg Laboratory in the early 1980's. Jumping robots are recently seeing increased attention for their ability to potentially navigate over obstacles that would stop a rolling or walking machine.

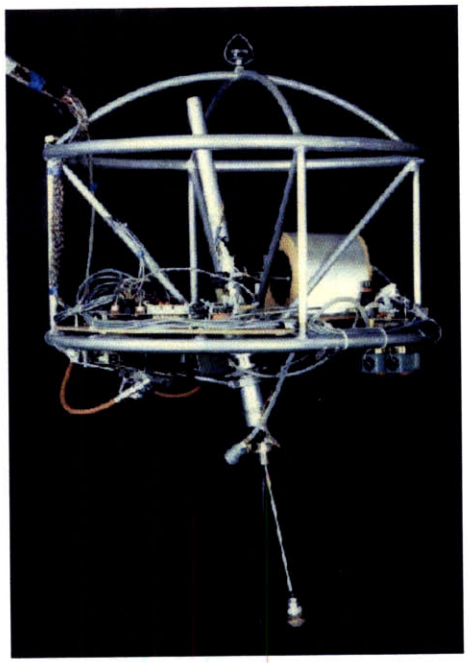

Figure 1. Raibert's 3D One-legged hopper. Raibert was a pioneer in the field of dynamic stability, and his early work focused mainly on jumping robots. Image taken from MIT Leg Laboratory, 1983 [3].

2.2 Linear Actuation

Most robots and other machines today use rotary actuators, most notable the DC motor. Linear actuators have the potential to reduce may problems seen with rotary actuators. Since most robots use DC motors, our discussion will focus on the comparison between linear actuators and DC rotary motors. DC motors are most efficient at high speeds and low torque. This situation calls for the use of gears that greatly reduce the speed of the motor output. Gears result in backlash, which causes positioning errors. Gears also cause a certain amount of energy loss.

Another reason to use linear actuators is their prevalence in nature. Skeletal muscles are linear actuators. If one desires to make a biologically-inspired robot, linear actuators are the natural choice.

Types of linear actuators include pneumatics, hydraulics, piezoelectrics, solenoids, and linear Lorentz-force actuators. Each of these has its advantages and disadvantages.

2.3 Parallel Actuation

When two or more independent actuators are connected to the same base and end effector, they are said to be in parallel. The alternative is to be in series, when one actuator is connected to another actuator which is then connected to an end effector. A leg is an example of a series architecture. The hip and waist connects to and actuates the thigh, which connects to the lower leg, which then connects to the foot. The eye is an example of a parallel architecture [4], shown in Figure 2. The Orbital muscles are connected to the skull and to the eyeball. They can, to some extent, operate independently of each other or they can operate together.

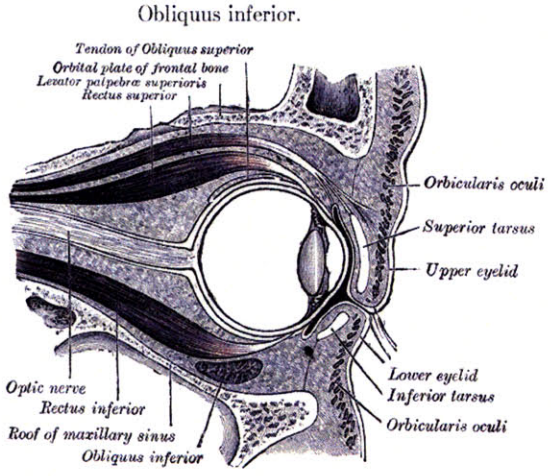

Figure 2. The Orbital Muscles in the human eye are arranged in a parallel architecture. This configuration contrasts almost all other muscles, such as the arms and legs, which are arranged in a series architecture. Image taken from *Gray's Anatomy*, 1962 [5].

Almost all mobile robots today use the series architecture. There are several advantages to using a parallel architecture instead of series. Series actuators have to support all of the links down the chain from themselves. This requires larger actuators, which then increases the loads even more. With parallel actuators, the load is distributed among several actuators, so the capacity is greater. In series architecture, the errors of the first links are magnified down the chain. In parallel architecture, this is not the case, and parallel architectures offer the advantage of increased resolution. Parallel structures are also stiffer than their series counterparts, because series structures suffer from more flexure in the links. For these reasons, a parallel architecture can be better than a series architecture.

Figure 3 shows the Gough tire testing rig and a schematic of the so-called Gough Platform [6]. This is today the most popular form of parallel mechanism for six degree-of-freedom motion. The platform uses six variable-length struts that can control the rotation and translation of the platform. Figure 4 shows an industrial positioning machine that uses the Gough platform (a) and a mobile robot (b) that uses the Gough platform for positioning of the feet.

Figure 5 shows a variety of two degree-of-freedom parallel systems. These systems use two actuated prismatic or revolute joints and three passive joints. They vary in the order and type of actuated and passive joints. For our robot, we will use three passive revolute joints and two actuated prismatic joints.

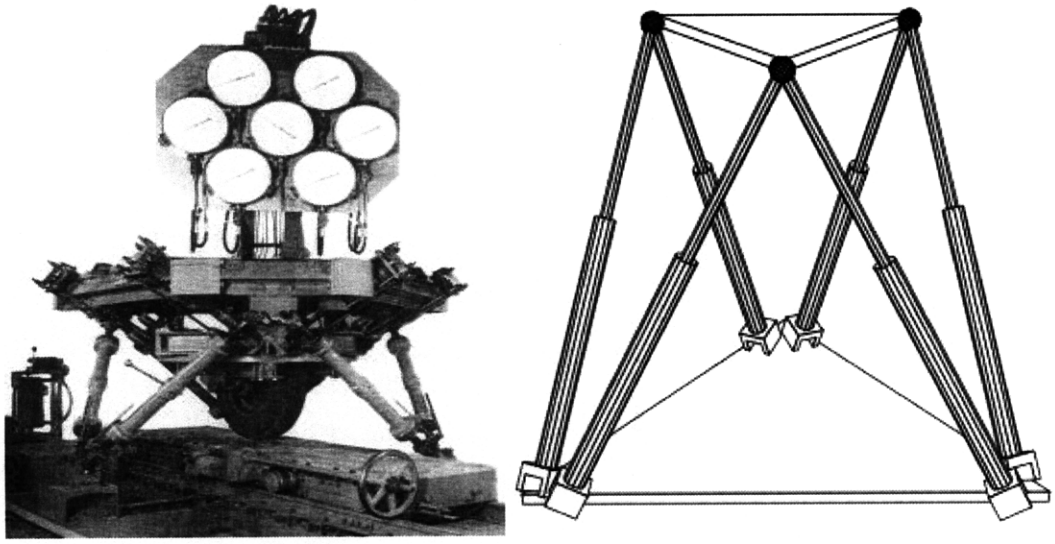

(a) (b)

Figure 3. The Gough Platform was developed by Dr. Eric Gough to test tires under various loading conditions. The platform is connected to six variable-length struts that give it six degrees of freedom. Images from *(a) Proc. IMechE*, 1965-66 [7]; *(b)* C.L. Collins, Univ. of California, Irvine.[8]

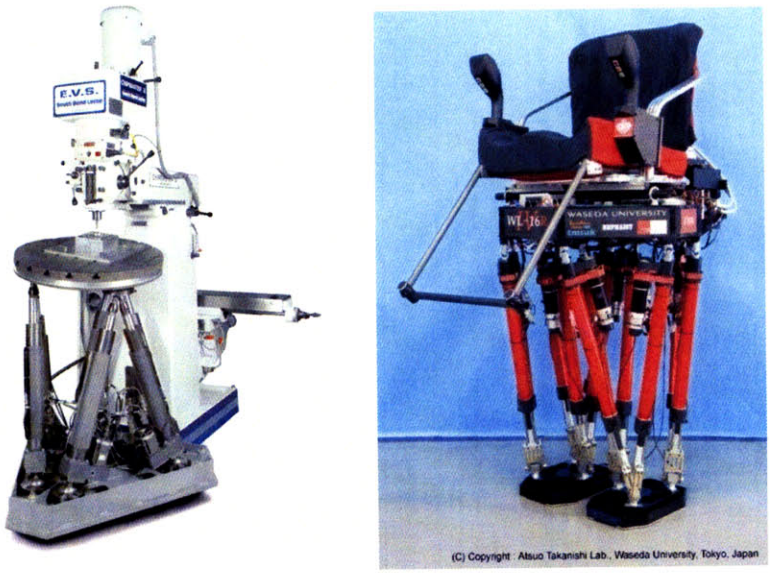

(a) (b)

Figure 4. Parallel actuators are becoming more common in industrial robots where high rigidity, repeatability and accuracy are required. Shown in (a) is the P2000 Hexapod Positioning System from Parallel Robotic Systems Corporation [9]. Some mobile robots, such as the Multi-purpose Biped Locomotor from the Takanishi Laboratory, also use parallel link actuators [10].

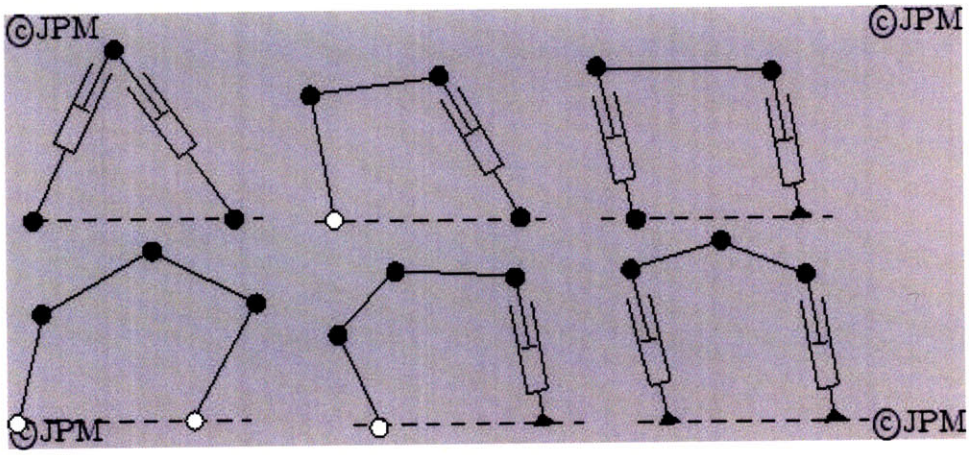

Figure 5. Various two degree-of-freedom parallel manipulators. These configurations use two actuated and three passive joints to obtain 2 DOF. Our robot is based off of the upper left design, which utilizes two actuated prismatic joints and three passive revolute joints. Image from *Parallel Robots*, by J.P. Merlet, 2006 [11].

2.4 Lorentz-Force Actuators

Lorentz-force actuators produce a force given by [12]

$$F = B \times I \tag{1}$$

where B is the magnetic field strength and I is the current flowing through the field. A Lorentz-force actuator consists of a magnet and a wire which usually makes many turns around the magnet. A higher force is produced from a stronger magnetic field or more turns of the wire. Figure 6 shows a cross-section of a linear Lorentz-force coil actuator, also known as a voice coil motor (VCM). This type of actuator is used in speakers to drive the speaker cone. VCMs are used in this application because of the very high speed at which they can operate, easily well into the kilohertz range. When a VCM is coupled with a displacement sensor, they have incredibly fine resolution, limited only by the sensing and driving devices.

From Equation (1), we see that the force is perpendicular to both the current and the magnetic field. As seen in Figure 6, careful orientation of the coil and magnet can ensure that the force is always in the desired direction. Also from Equation (1), we see that the force produced is linear with the current. This property makes VCMs very controllable. Their bandwidth is limited mainly by the inductance of the coil and the inertia of the moving mass.

Lorentz-force actuators are very efficient at converting electrical energy to mechanical energy. The main form of energy dissipation is friction in the bearings used to align the coil with the magnet. The main drawback of VCMs is their relatively short stroke length. This distance can be increased by increasing the length of the magnet or coil, however this reduces the power-to-weight ratio. Despite this drawback, Lorentz-force actuators are suitable for many applications where a large stroke is not required.

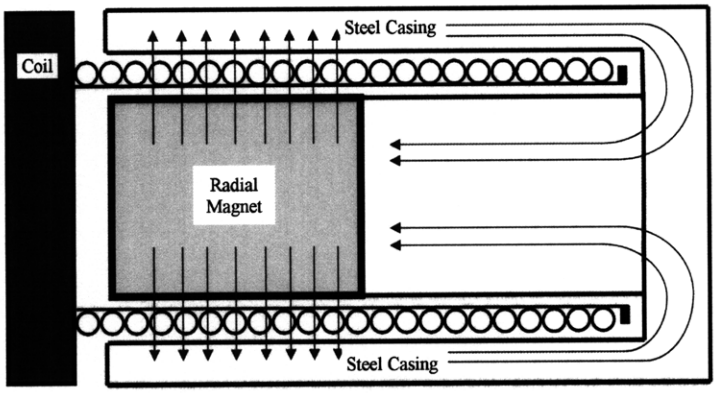

Figure 6. Cross-section of Lorentz-force motor with magnetic field lines illustrated. The magnet creates a B-field that is always perpendicular to the current flowing through the coil. This produces a force in the direction given by the cross-product of the B-field and the current. (Based on Taberner et. al., 2006 [13]).

3.0 Theoretical Approach

3.1 Fundamental Requirements

To determine the correct approach for the design of the robot, we first determined some basic design parameters that the robot will follow. The maximum mass of the robot was set at one kilogram. In addition, the overall height should be approximately 150 mm, which will keep the robot in the range suitable for operation on a desk or work bench. These constraints were created to maintain the design and construction at a reasonable level of cost and complexity, as well as to allow use of the robot in the space available in the laboratory.

The goal of the robot was to be able to jump at least 15 mm, using actuators with a 15 mm stroke length. The jump height and stroke length were determined based on the desired size of the robot, as well as to set the goal of having the robot jump to a height equal to its stroke length.

Another design parameter is that the robot is to operate only in a single, two-dimensional plane. This reduces the complexity of the project by requiring only two actuators. To confine the robot to only horizontal (in one direction) and vertical translations reduces the degrees of freedom from six to two. A suitable constraint apparatus would be designed to reduce the possible motions of the robot to only these two translations.

One more decision about the design of the robot concerned the ability of the robot to balance. This problem was determined to be unnecessary to the scope of this project, as it is already known that dynamic stability is possible with jumping robots. Also, the inclusion of the balance problem would substantially increase the complexity of the project.

The parallel architecture was determined because of the advantages discussed earlier. This configuration would likely offer the best combinations of controllability, power, precision, and speed that we desire for a high-performance robot.

In summary, the design parameters of this project are to build a two degree-of-freedom jumping robot that uses linear Lorentz-force actuators arranged in a parallel architecture. The actuators should have a stroke length of approximately 15 mm, which should allow it to jump to a height of 15 mm. The total mass of the robot should be approximately one kilogram, and it should be about 150 mm in height.

3.2 Geometrical Design

With the design parameters set, the next step is to determine the geometry of the robot, and then to determine the behavior of the robot with this geometry. The final design is shown in Figure 7. The design consists of a triangle shape with two actuators residing on opposing sides and a rigid base above. With this design, the actuators can exert force in both the horizontal and vertical directions. The symmetry of this design allows pure vertical motion by actuating the motors with equal current. Horizontal motion can be achieved by actuating one motor more than the other.

The location of the foot can be solved with only knowledge of the actuator displacement, the unextended leg lengths, and the base length. With this information, the lengths of the three sides of the triangle are known, and the position of the foot can be solved using the Law of Cosines. The foot location is given by the following equation, where X_1 is the vertical displacement, X_2 is the horizontal displacement, L_a is the length of the base, L_b is the unextended length of Leg B, L_c is the unextended length of Leg C, q_b is the displacement of the motor on Leg B, q_c is the displacement of the motor on Leg C and θ_c is the angle between Leg B and the base. (2)

$$X_1 = -(L_b + q_b) \cdot \sin(\theta_c) \tag{3}$$

$$X_2 = (L_b + q_b) \cdot \cos(\theta_c)$$

where

$$\theta_c = \cos^{-1}\left[\frac{{L_a}^2 + (L_b + q_b)^2 - (L_c + q_c)^2}{2L_a(L_b + q_b)}\right] \tag{4}$$

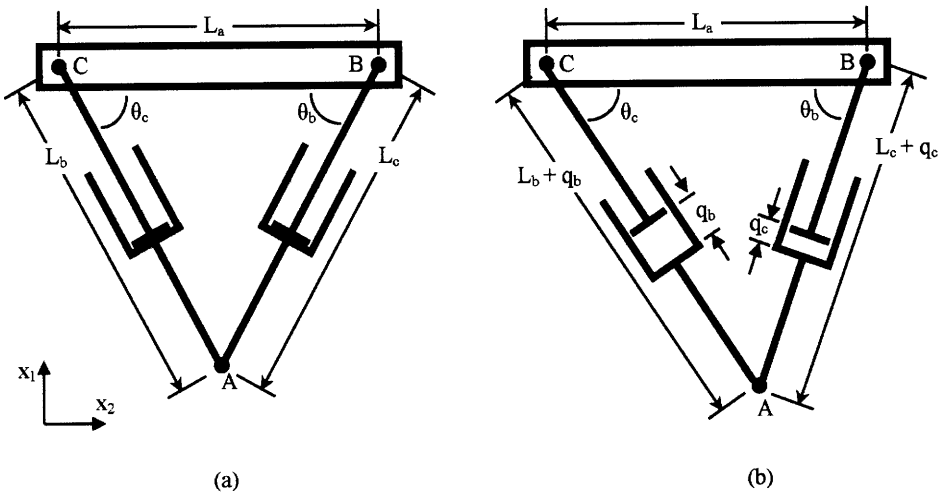

Figure 7. Geometry of robot in unactuated (a) and actuated (b) positions. The position of the foot, point A, is determined from the actuator displacement, the base length the unextended leg lengths (L_a, L_b, and L_c)

With the foot location known, we can optimize the lengths of the legs based on the maximum range that the legs can move. A MATLAB script (Appendix 1) was written that uses Equations 2, 3, and 4 to solve for the location of the foot for all possible actuator displacements. From this, we obtained a plot of vertical and horizontal range as a function of the ratio of the leg length to the base length. For simplicity, it was assumed that the actuated legs had the same unextended length. The result is shown in Figure 8. The horizontal range increases linearly with increasing leg length. The vertical range, however, quickly approaches a lower limit equal to the maximum motor displacement. This result indicates that a huge horizontal range could be achieved by making the legs very long, however intuition tells us that if the legs are very long compared to the body, the motors will be nearly vertical, and thus not able to exert much force in the horizontal direction. Next, an analysis was conducted to determine the effect of leg length on horizontal and vertical force.

The force available for motion in either the horizontal or vertical direction is a function of the magnitude of the motor force and the angle at which the motors act. The forces are given as

$$-F_1 = F_b \sin\theta_c + F_c \sin\theta_b \quad , \tag{5}$$

$$F_2 = F_b \cos\theta_c + F_c \cos\theta_b \quad , \tag{6}$$

where F_1 is the vertical component of the force, F_2 is the horizontal component, and F_b and F_c are the forces from the motors on legs B and C, respectively. The forces depend on the leg length through the dependence on the angle of the legs. Figure 9 shows the available motion force per unit actuation force as a function of the leg length body length ratio. The results show that, as expected, the horizontal force decreases with leg length and the vertical force increases with leg length.

With the information from Figures 8 and 9, we can decide on a suitable leg length ratio. Because the robot will have to contend with gravity, we conclude that more vertical force is required than horizontal force. The plot of range shows us that the vertical range will not be much greater than the actuator displacement for any leg length that gives a reasonable vertical force. Thus we conclude that we should pick a ratio that does not jeopardize the horizontal force. A length ratio of unity was chosen because at this ratio, the horizontal force is approximately equal to the force generated from a single motor, and the vertical force is nearing its limit. Thus, the legs will be equal in length to the base.

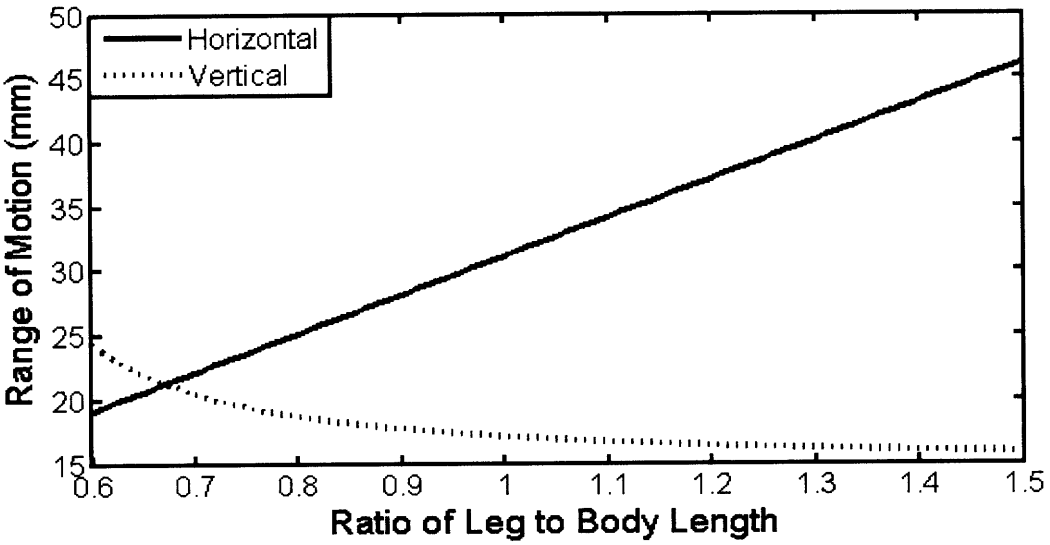

Figure 8. Range of motion as a function of the leg length - body length ratio. Here, the maximum actuator displacement is 15.1 mm. The Horizontal range increases linearly with leg length, while the Vertical range asymptotically approaches the value of the maximum actuator displacement.

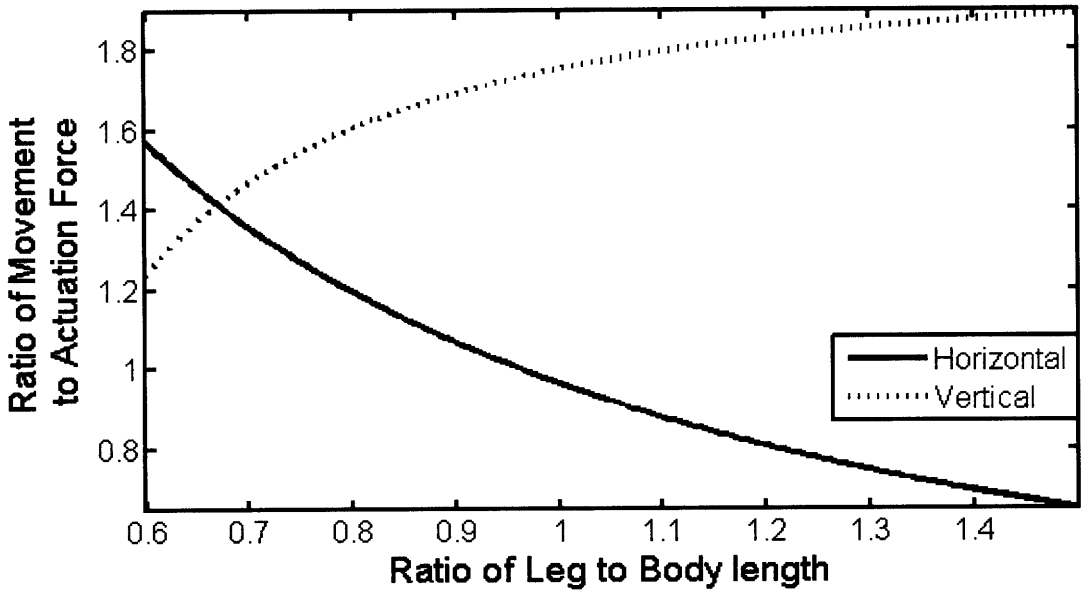

Figure 9. Movement force as a function of the leg length - body length ratio. The movement force is defined as the force available from the actuators in the vertical and horizontal directions, respectively. This force is determined from the angle between the legs and the ground. The horizontal force decreases with leg length, while the vertical force increases with leg length.

3.3 Jump Model

Figure 10 shows the sequence that the robot undergoes while jumping. Initially, the robot is at rest, with the motors fully retracted. When a current is applied to the motors, they extend at a constant acceleration. At this point, the foot is still on the ground. When the motors are fully extended, they collide with a hard stop in the bearing system that prevents the motors from extending any farther. Because the motors and base have inertia, they continue to move up, pulling the foot off of the ground. The robot moves to some maximum height before it returns to the ground. When the foot hits the ground, it pushes the motors closed. The robot is then ready for another jump.

Position sensors can be used to determine which state the motors are in at any time. This feedback would tell the controller when another jump is possible. Also, energy could be saved by not forcing the motors when they are fully extended. When the motors are fully extended, they cannot exert a useful vertical force on the robot, although sending current to them expends energy.

The jump height can be determined from application of the law of conservation of energy. The electrical energy input to the system is converted to mechanical energy in the form of kinetic and potential energy. When the robot is at its maximum height, all the input energy (minus losses) is in the form of gravitational potential energy. With this analysis, we can determine what current is necessary to make the robot jump.

We start with the weight of the robot, $mg = (1\ kg)(9.8\ m/s^2)$. As a rule of thumb, we want ten times this weight in vertical force to make to robot jump. Thus, we require approximately $100\ N$ of vertical force. With the motors angled at 60 degrees, we require 58 N from each motor. The force constant of our motor is $3.75\ N/A$. This gives us a required current of $(58\ N) / (3.75\ N/A) = 15\ A$. The resistance of the coil is 5 Ω, giving a voltage of $(15\ A)(5\ \Omega) = 75\ V$. Thus, the electrical power input is $(15\ A)(75\ V) = 1125\ W$.

The potential energy of the system, is given as

$$PE = (Lower\ Mass + Upper\ Mass) \cdot g \cdot h + (Upper\ Mass) \cdot g \cdot x$$

where the masses are as shown in Figure 11 and x is given as the vertical displacement of the motors.

As an estimate, half the mass will be in the top and half in the bottom. The vertical displacement will be the actuator displacement times $sin(60)$. Thus, the potential energy when the foot is 15 mm off the ground is equal to $(0.5\ kg+0.5\ kg)(9.8\ m/s^2)(0.015\ m)+(0.5\ kg)(9.8\ m/s^2)(0.015\ m)(sin(60)) = 0.21\ J$.

To get 0.21 J into the system, we need to apply the computed voltage for 0.21J/1125W=0.18 ms. This time will need to be divided by our efficiency. For fifty percent efficiency, this gives 0.36 ms. Thus to jump 15 mm, we need to apply 75 volts to the motors for 0.36 ms.

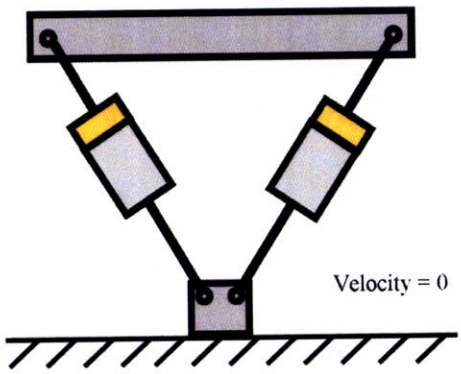

(a)

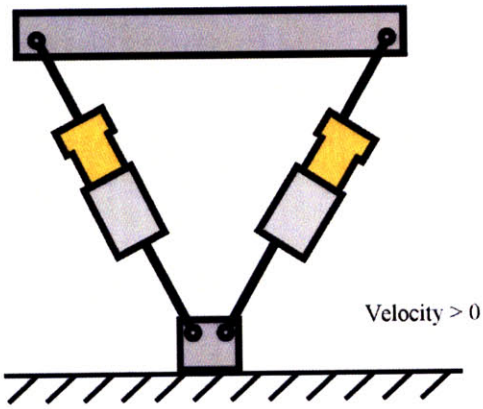

(b)

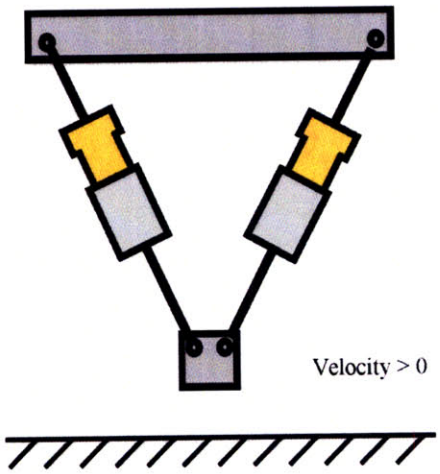

(c)

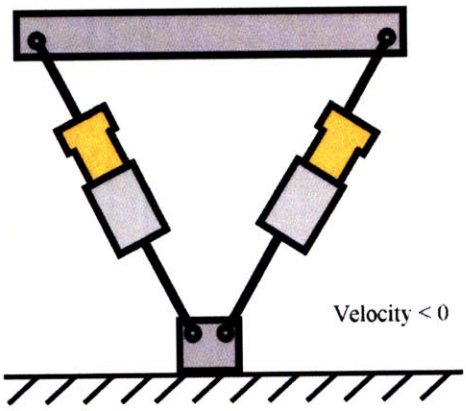

(d)

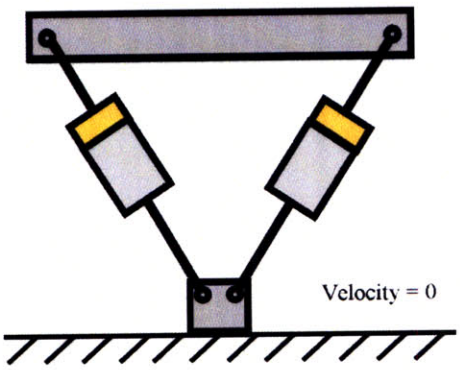

(e)

Figure 10. *Robot jump sequence. The robot begins in the standing position with the motors fully retracted (a). The motors actuate and the legs extend (b). When the legs are fully extended, the inertia of the body carries the legs off of the ground (c). Upon landing, the foot contacts the ground with the motors still extended (d). Then, the mass of the body forces the motors to close (e). We are now ready for another jump. Position sensing of the motor displacement allows the control program to know when the robot has landed.*

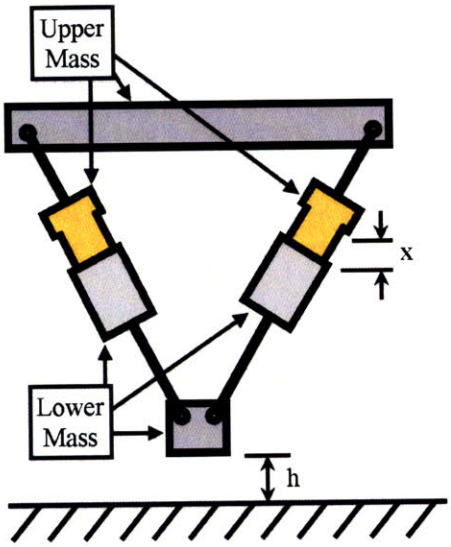

Figure 11. Robot potential energy. The gravitational potential energy of the robot depends on the height of the foot from the ground, as well as on the magnitude of the actuator displacement.

4.0 Design and Fabrication

4.1 Mechanical Design

4.1.1 Motor Selection

The first step in the mechanical design is the selection of a motor, and we will build the rest of the machine around the motors. Our most stringent requirement is that the motor have a stroke length of approximately 15 mm. After that, we want a motor with the best power to mass ratio and capable of producing the required force. With a mass limit of one kilogram, we cannot afford to get motors that are more powerful than we require. The motor that we selected is Model LVCM-025-029-01 from Moticont [14]. The motor has a stroke of 15.2 mm, a rated peak force of 16 N, and a mass of 105 g. Note that the peak force is the maximum force at a ten percent duty cycle. We will operate at a substantially lower duty cycle, so we can get a higher peak force without damage to the coils.

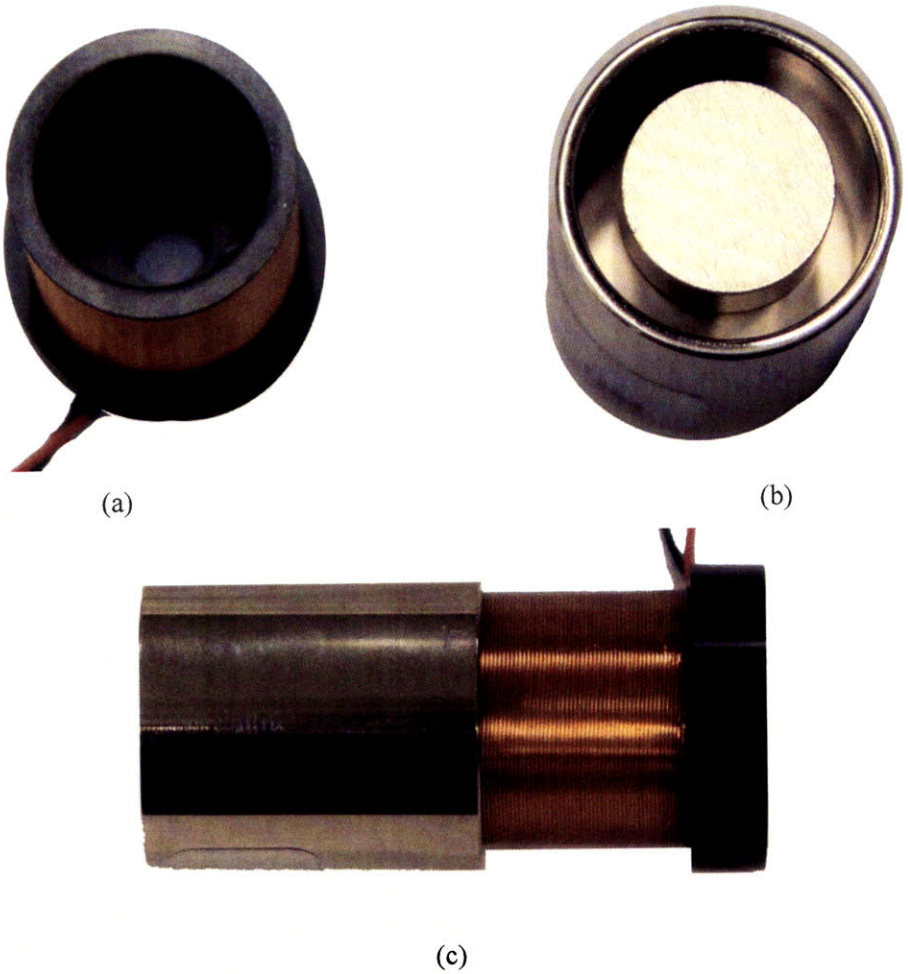

Figure 12. Lorentz-force motors used in the robot. The coil (a) slides into and out of the magnet (b) as seen in (c).

4.1.2 Other Parts

Figure 13 shows the parts that will make up the robot. The coil is attached to the upper motor mount, which attaches to the upper leg with the upper connector. The upper leg attaches to the base through a pin joint. The magnet attaches to the lower motor mount, which attaches to the lower leg with the lower connector. The lower leg attaches to the foot with a pin joint.

One requirement for the motor is that it must be constrained axially, and it cannot support a bending or radial load. Rails and sleeve bearings were designed to constrain all five unwanted degrees of freedom. They are arranged in a symmetric pattern at the corners of an equilateral triangle. The bearings are threaded to attach to the lower motor mount. The rails are threaded and fit into the upper motor mount block. The other end of the rails is threaded to hold a nut that will prevent the coil from moving outside of the magnet. Figures 14 and 15 show photographs of the motor mounts with and without the motors connected.

To connect the motor mounts to the motors, we use the threaded holes that were prefabricated into the magnet and coil. The connectors attach to the motor mounts and are threaded to connect to the legs. Figure 16 has photographs of the connectors with the legs attached.

One issue that was encountered during design was a way to keep the foot oriented toward the ground while still allowing free rotation of the legs. This problem was solved by adding torsion springs as a preload to the legs. The springs keep the foot oriented at the bisection of the angle between the legs. The springs do not reduce the force from the motor because as one spring stores energy, the other releases energy, so they balance each other. This mechanism can be seen in Figure 17.

A high-friction, soft rubber pad was attached to the foot, as seen in Figure 18. This pad serves two purposes. It absorbs shocks as the robot impacts the ground and helps the robot to grip the ground so the foot does not slip out from underneath it.

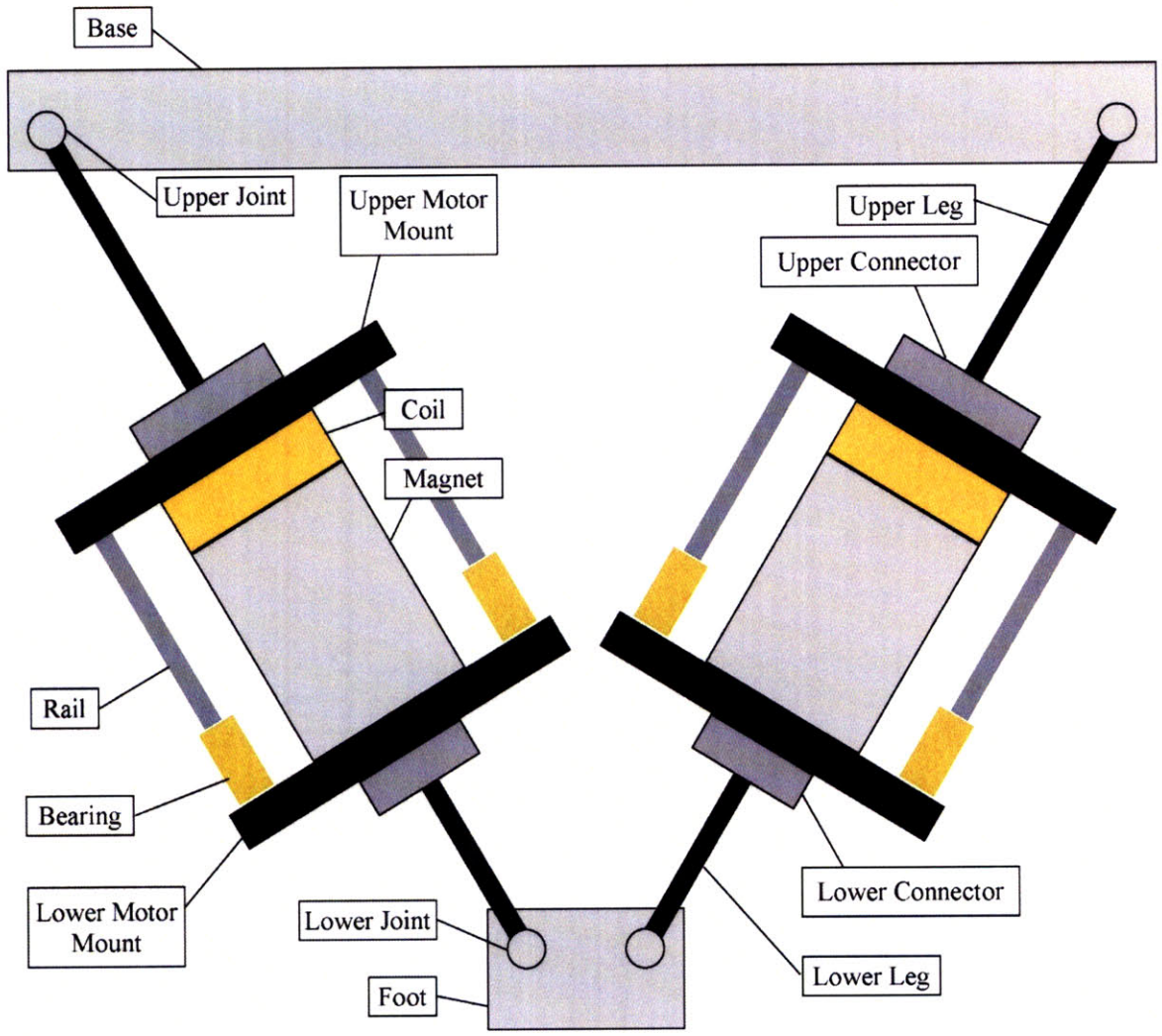

Figure 13. Robot design and individual parts identification. The Rails and Bushings constrain the motor to axial motion. The Upper and Lower Joints are passive revolute joints that allow the footpad to assume a position based on the actuator displacements. The Foot contains torsion springs which keep the foot oriented at the bisection of the angle between the two legs. The Base provides a rigid support for the legs and connections to the balance mechanism, discussed below.

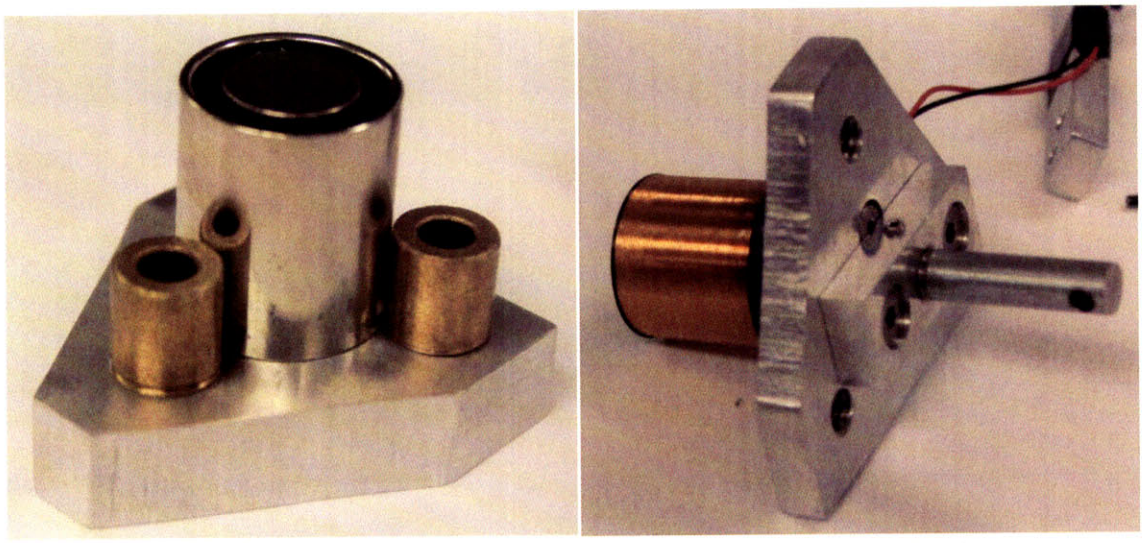

Figure 14. Lower and upper motor mounts with motors connected. The magnet and coil came supplied with mounting holes to which the motor mounts connect.

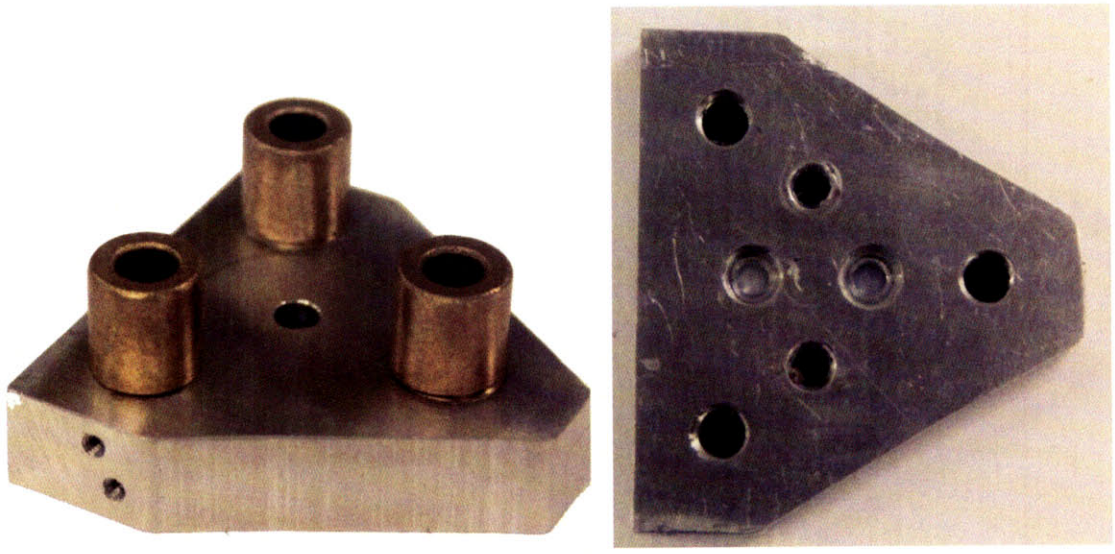

(a) (b)

Figure 15. Lower (a) and upper (b) motor mounts. The mounts also connect to the bearings and rails, which provide constraint in all motions except for axial motion, keeping the coil aligned within the magnet.

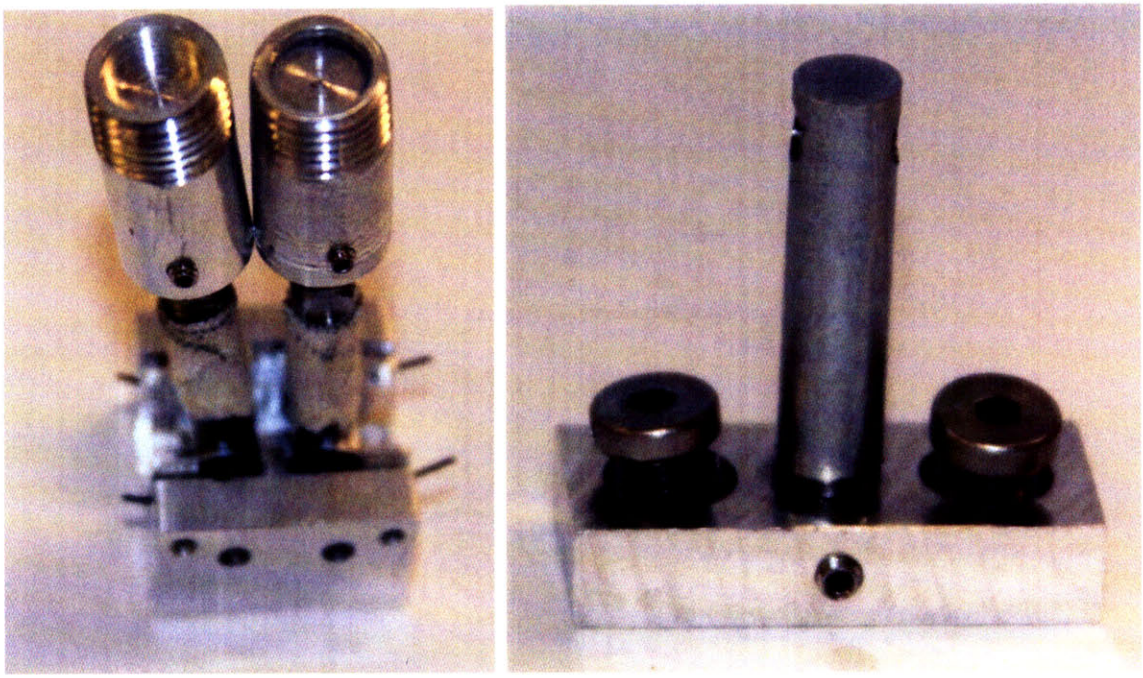

(a) (b)

Figure 16. Lower (a) and Upper (b) connectors with legs attached. The lower and upper connectors connect the motor mounts to the lower and upper legs, which connect to the foot and base, respectively.

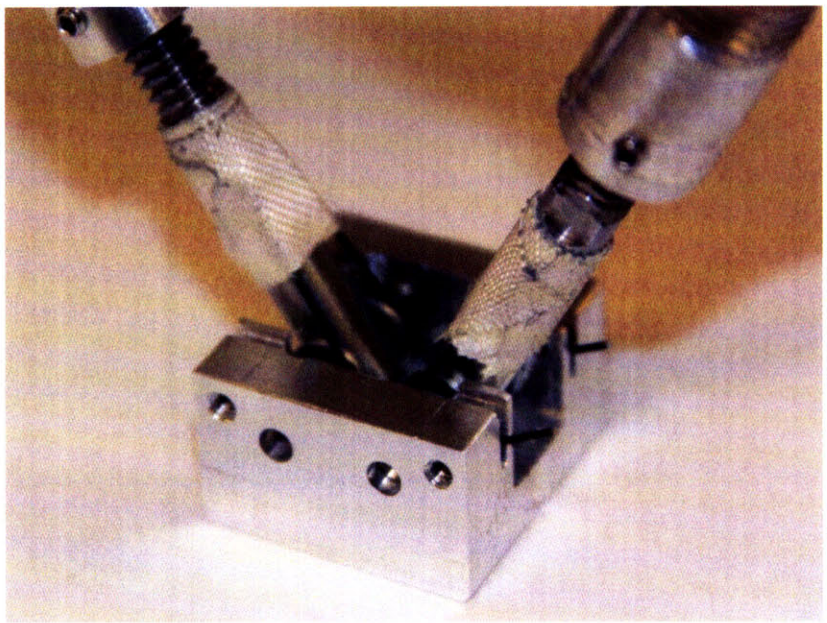

Figure 17. The foot connects to the lower legs and allows rotation through the use of pin joints. Torsion springs keep the foot oriented toward the ground.

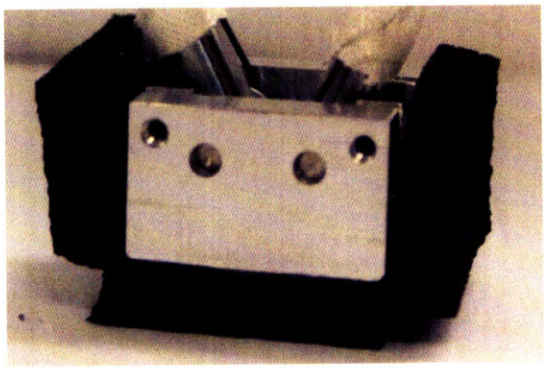

Figure 18. A rubber pad is adhered to the foot to provide shock absorption and a high friction surface.

4.1.3 Constraint and Balance Apparatus

The robot cannot balance itself, so we need a device that will hold the robot in the vertical position. Seen in Figure 19 is the device designed to provide balance to the robot. The device is a set of legs that extend the support polygon to surround the center of mass of the robot. This device does not constrain the motion of the robot other than preventing it from tipping over. Balancing the robot proved to be sufficient to allow for testing of the maximum jump height.

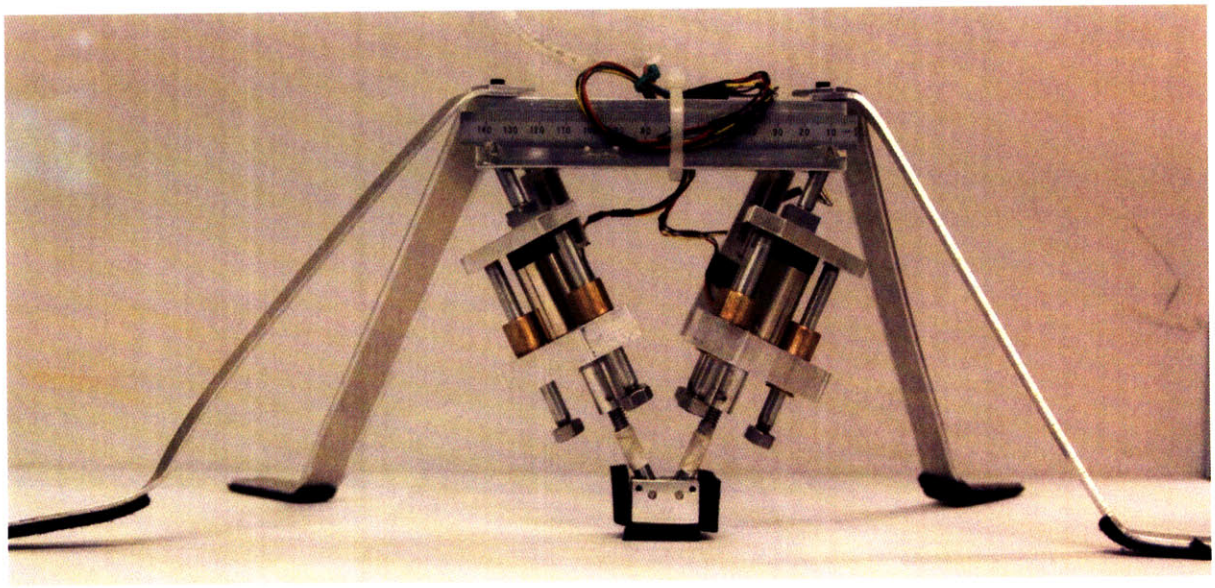

Figure 19. Four support legs were added to keep the robot from falling. This approach was used after the planar motion constraint devices failed to perform adequately.

4.2 Electrical Design

4.2 1 Power Switching

As shown previously, we desire a large amount of current to flow into the motors for a short, controllable period of time. We used IXYS TrenchT2 power MOSFETS [15] to perform the switching, in conjunction with MOSFET drivers and digital input from a computer-controlled NI-DAQ unit. The circuit schematic for a single motor is shown in Figure 20. An identical circuit was also used for the other motor. The motors were connected in parallel to the same power supply.

The circuit works by connecting the leads of the motor to the pins labeled *VCM+ and VCM-*. When the MOSFET is off, its resistance is very high, and the motor sees an open circuit. When the MOSFET switches on, its resistance gets very low and the motor has a connection between the positive power supply voltage and ground, so current flows and the motor causes the robot to jump. The switching of the MOSFET is powered by the driver, which amplifies the signal from the DAQ to be able to quickly switch the MOSFET. This circuit also contains two diodes which act to protect the motor and MOSFET from voltage spikes. The components were soldered to a prototyping board with banana jacks for external connections. The board is shown in Figure 21.

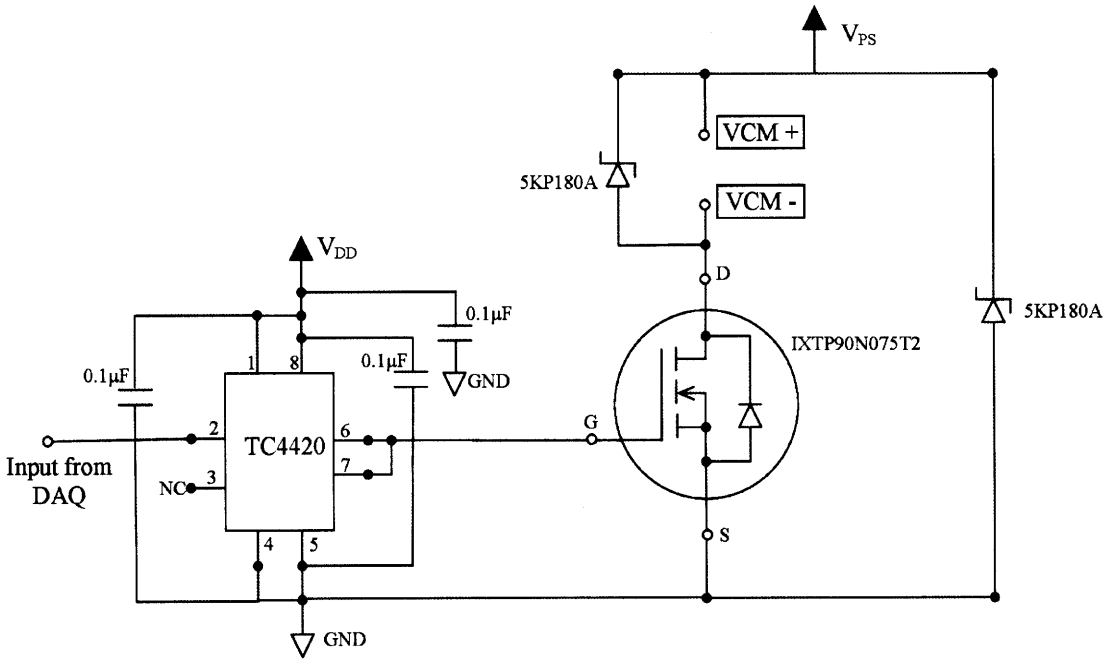

Figure 20. Electrical circuit used to drive the motors. The controller sends a signal to the driver, which amplifies the signal and sends it to the power MOSFET. The MOSFET switches the motor on or off. The voltage sent to the motors is V_{PS}.

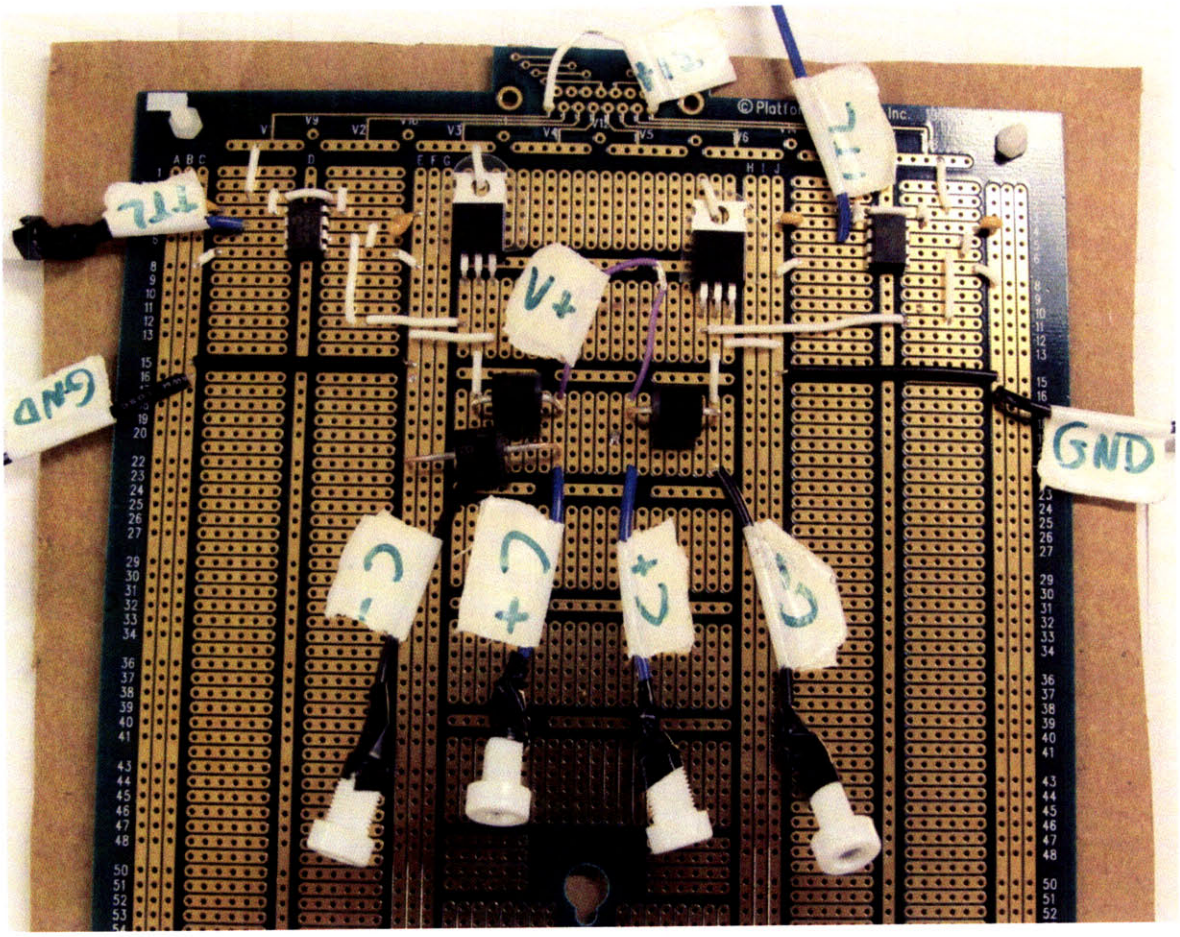

Figure 21. Photograph of the control circuit. A separate driver and MOSFET is used for each motor. Both motors use the same power supply voltage, connected at V+.

4.2.2 Power Sources

The electrical circuit required two separate supply voltages. The MOSFET drivers were supplied with 6 V with the Agilent E3631A [16], shown in Figure 22. The motors required a much higher voltage and current than this power supply could provide. For this, we used the Agilent E4356A [16], which can output 80 V at up to 30 A. This power supply is shown in Figure 23.

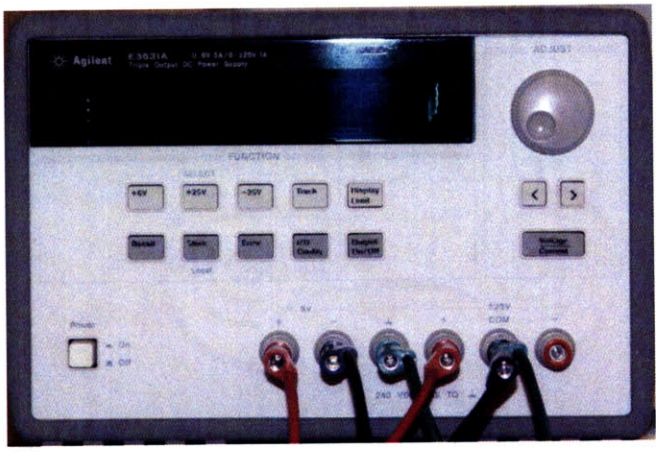

Figure 22. Photograph of the power supply used to power the driver. A 6 V signal was used.

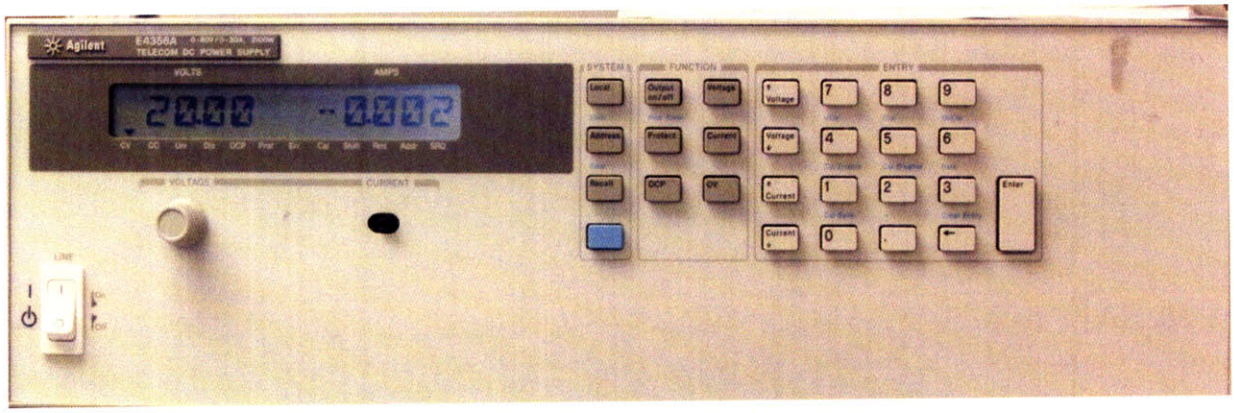

Figure 23. Photograph of the power supply used to power the motors. This PS is capable of 80 V and 30 A. The motors were powered at up to 70 V.

Figure 24. Photograph of the National Instruments Data Acquisition Unit, the DAQPad 6052e. This device contains digital I/O lines and analog input and output ports.

4.2.3 Digital Control

To command the MOSFET driver, we used LabView interfaced with the National Instruments Data Acquisition Unit shown in Figure 24. This device, the DAQPad 6052e [17], contains digital I/O lines which we used to send command signals to the driver. A logical high would switch the MOSFET on, thus driving the motor, while a logical low would turn off the MOSFET and the motor.

To control the DAQ, we used the LabView VIs shown in Figures 25, 26, and 27. Figure 25 shows the VI that sends the DAQ output high on two channels. A similar VI was used to send the outputs low. These two VIs, "On" and "Off" were embedded inside a VI that the user could interact with. Figure 26 shows the front panel of the VI that causes the robot to jump. The user inputs a desired pulse duration, which is how long the motor will stay on. The "Jump" button initiates the jump. The block diagram for this program is shown in Figure 27.

Figure 28 shows an oscilloscope reading of the DAQ output lines when a command of one millisecond is sent. The line goes high to 5 V for 1 ms before returning to ground. This would send current to the motors for 1 ms.

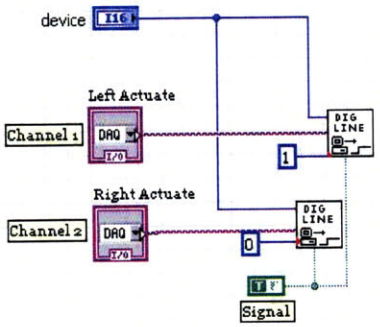

Figure 25. The LabView block diagram used to turn on the motors. To turn off the motors, the signal is changed to "false".

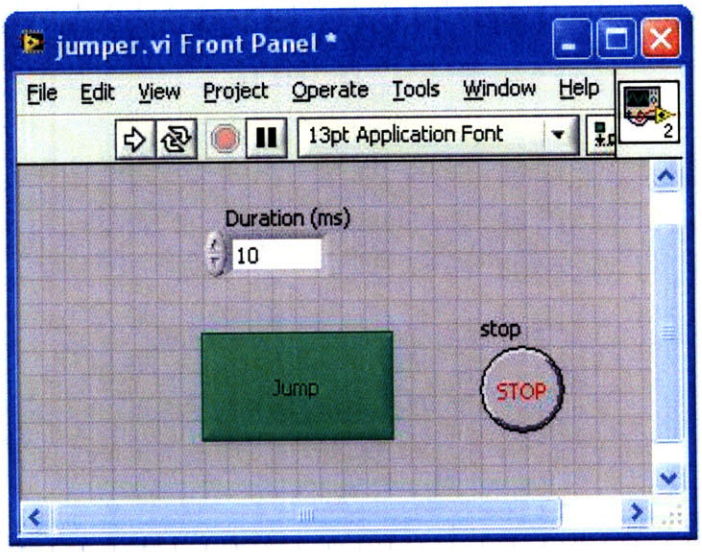

Figure 26. The LabView front panel used to control the motors. The user sets the duration of the pulse of current to be sent to the motors. The "Jump" button initiates the jump.

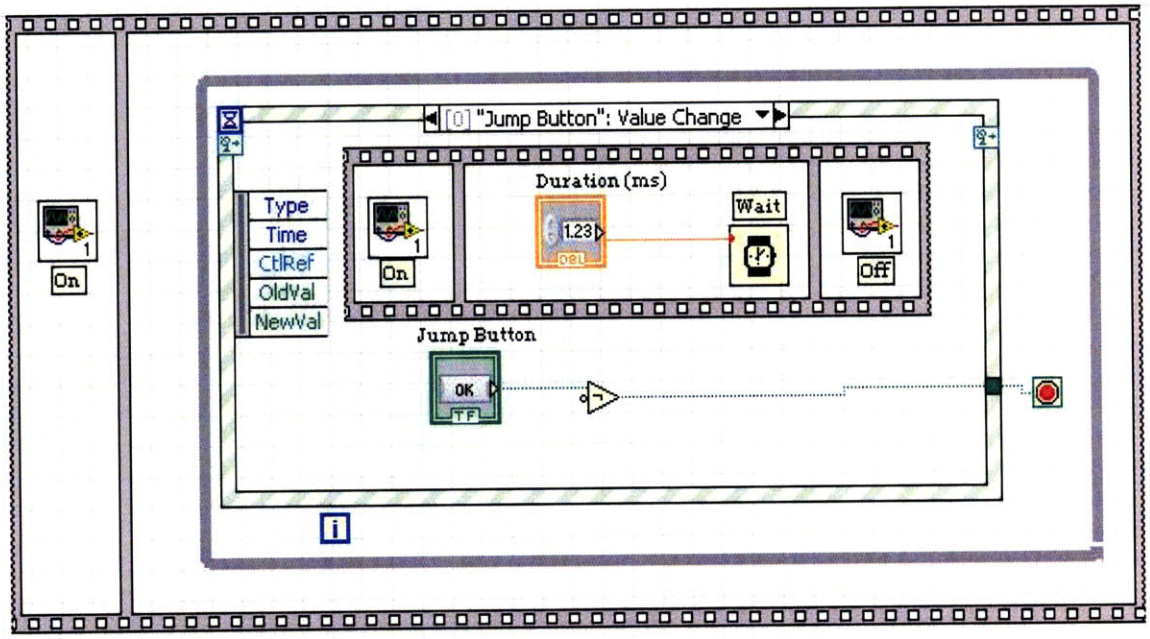

Figure 27. The LabView block diagram used to control the motors. The FP reads the user-input duration and sends the jump signal when the "Jump" button is pressed.

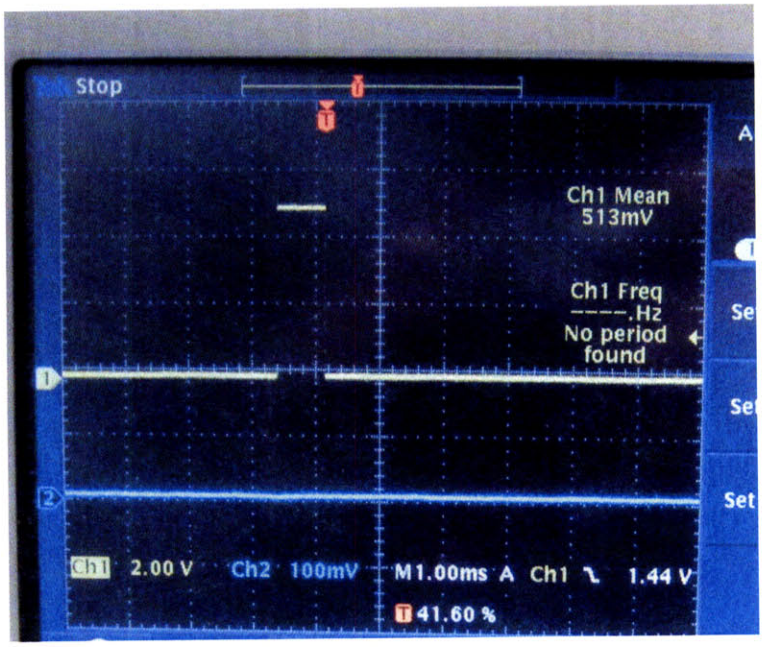

Figure 28. An oscilloscope reading of the signal sent to the motors. For this signal, the user-defined duration was set to one millisecond. The scope confirms that the signal is being sent for the correct length of time.

5.0 Results

Our results are shown in Figure 29 in a plot of jump height as a function of pulse duration for three voltage inputs. These values were taken images captured using the Phantom v9.0 high-speed camera from Vision Research, Inc. [18]. An example of a jump is shown in Figures 30-35. Our results show a linear relationship between pulse duration and jump height, which is consistent with our theory, since the energy input to the system varies linearly with time and the height of the jump varies linearly with energy input. After a certain point, however, the jump height stops increasing with pulse duration. This point corresponds with the motor reaching the end of its stroke. At this point, no more energy can be input to the system; hence the jump height is not altered by turning on the motors beyond this point. The jump height also increases with supply voltage, again consistent with our theory. Data was obtained for voltages up to 60 V. When a 70 V supply was used, the MOSFETs failed.

The maximum recorded jump height was 46.1 mm, at 60 V for 15 ms. The average jump height for a 60 V supply at pulse duration of 15ms or greater was 44.9 mm. This value is significantly higher than our goal of 15 mm.

The pulse durations were significantly higher than the estimated duration at 75 V to jump 15 mm. Longer durations were used for two reasons. First, the circuit could not withstand 75 V, so lower voltages were used. This lowered power input to the system, which meant that longer pulse durations were required. Second, longer durations were used to enable the robot to jump higher than the goal of 15 mm.

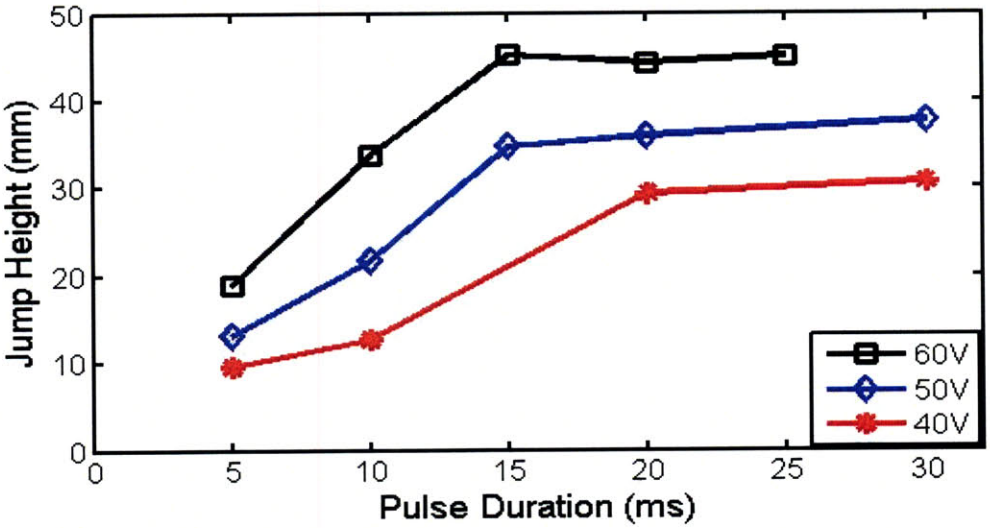

Figure 29. Average Jump height as a function of pulse duration for various driving voltages. The height-duration relationship is linear until the duration extends beyond the time that the motors are fully extended. When the motors are fully extended, no more energy can be put into the system.

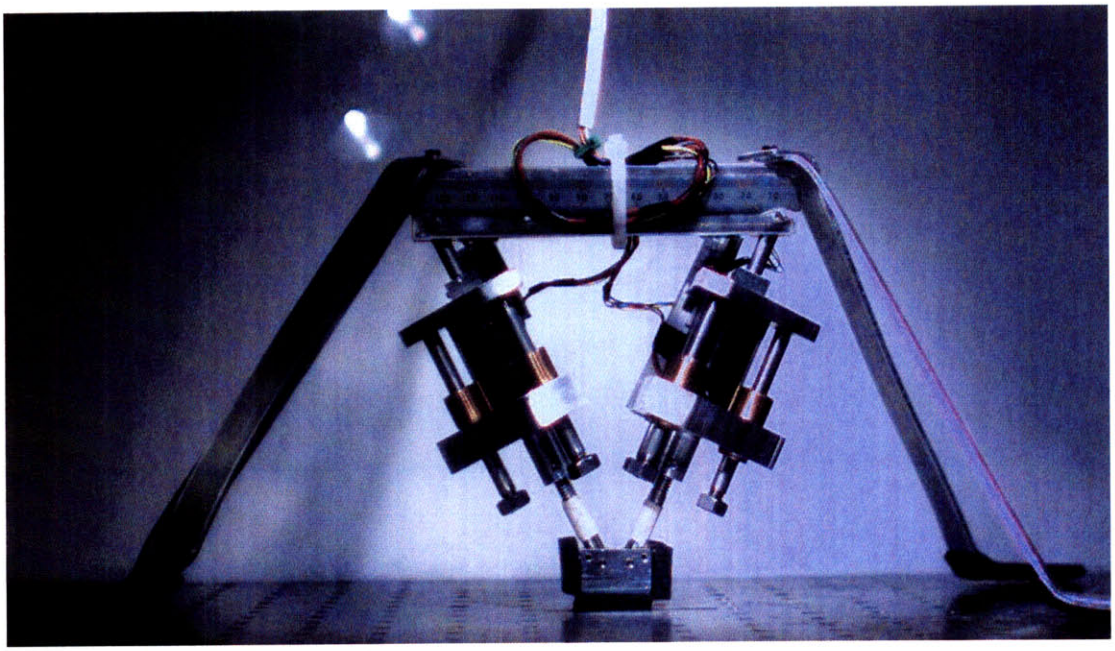

Figure 30. High speed camera image of jump – standing. This picture was taken before the jump signal was sent to the motors.

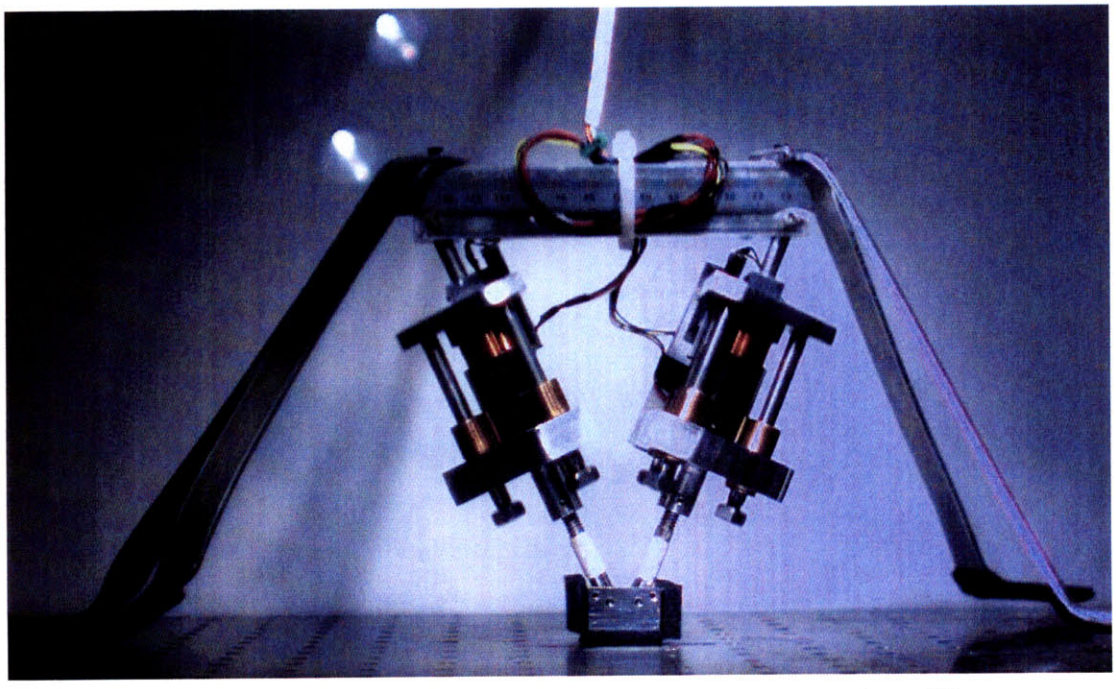

Figure 31. High speed camera image of jump – partial extension. This picture captures the extension of the motors before they are fully extended. The robot will remain on the ground until the motors reach the end of their travel.

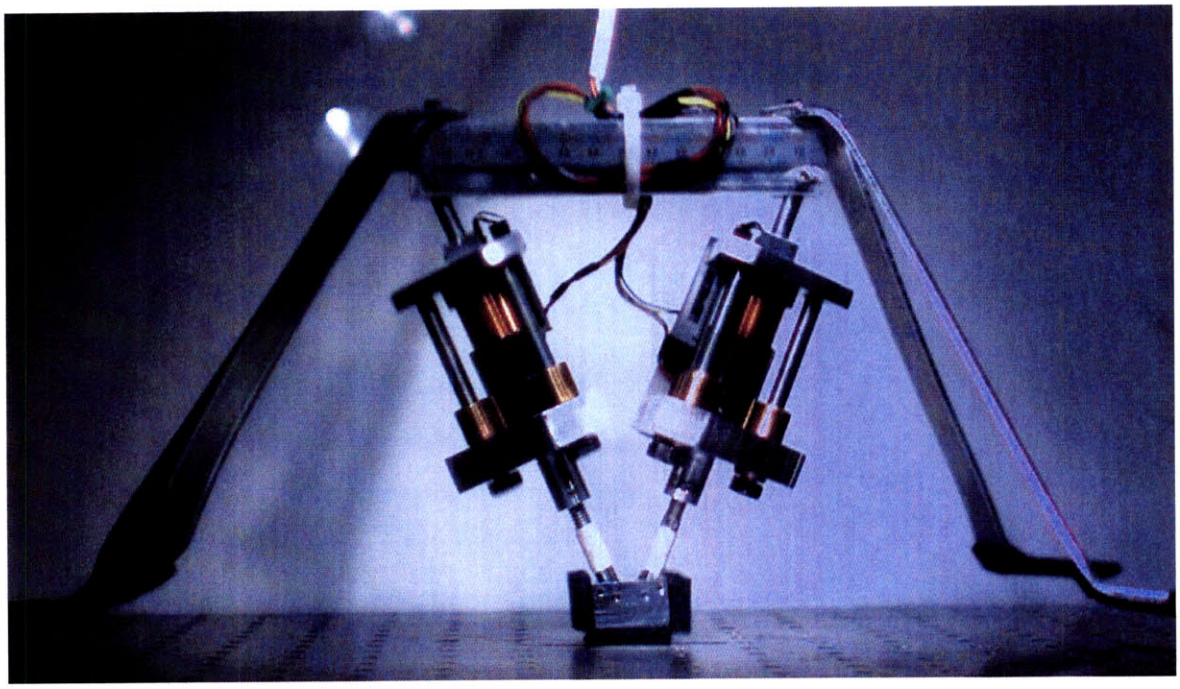

Figure 32. High speed camera image of jump – full extension. This photograph shows the motors fully extended but still on the ground.

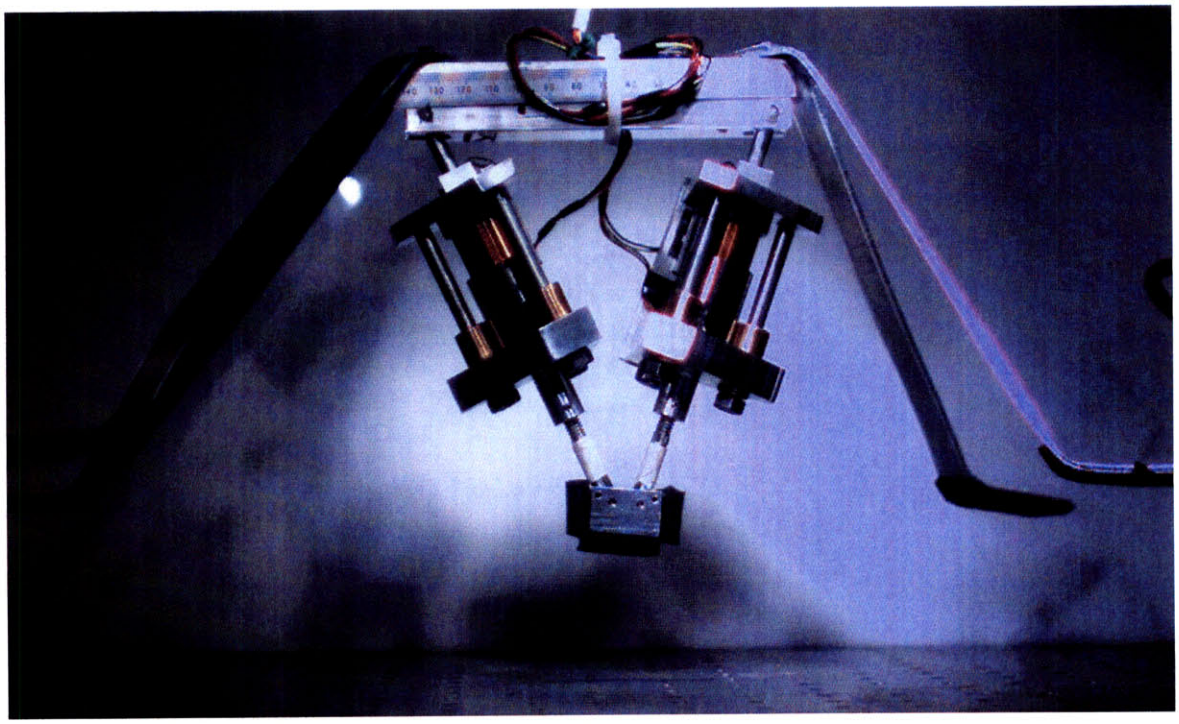

Figure 33. High speed camera image of jump – jumping. The robot is at its maximum jump height. There is no current flowing through the motors at this point, however they will stay fully extended until the robot returns to the ground.

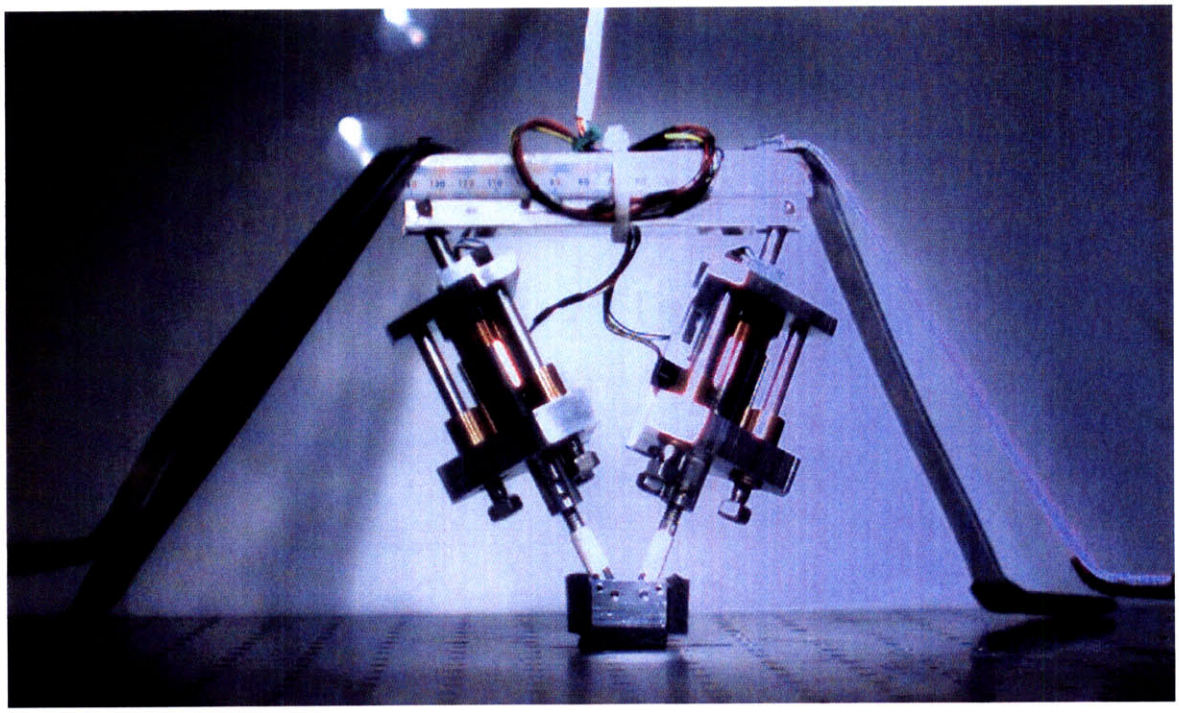

Figure 34. High speed camera image of jump – landing. The robot has returned to the ground and the motors are beginning to retract. This retraction can be monitored by the displacement sensors to know that the robot has touched down.

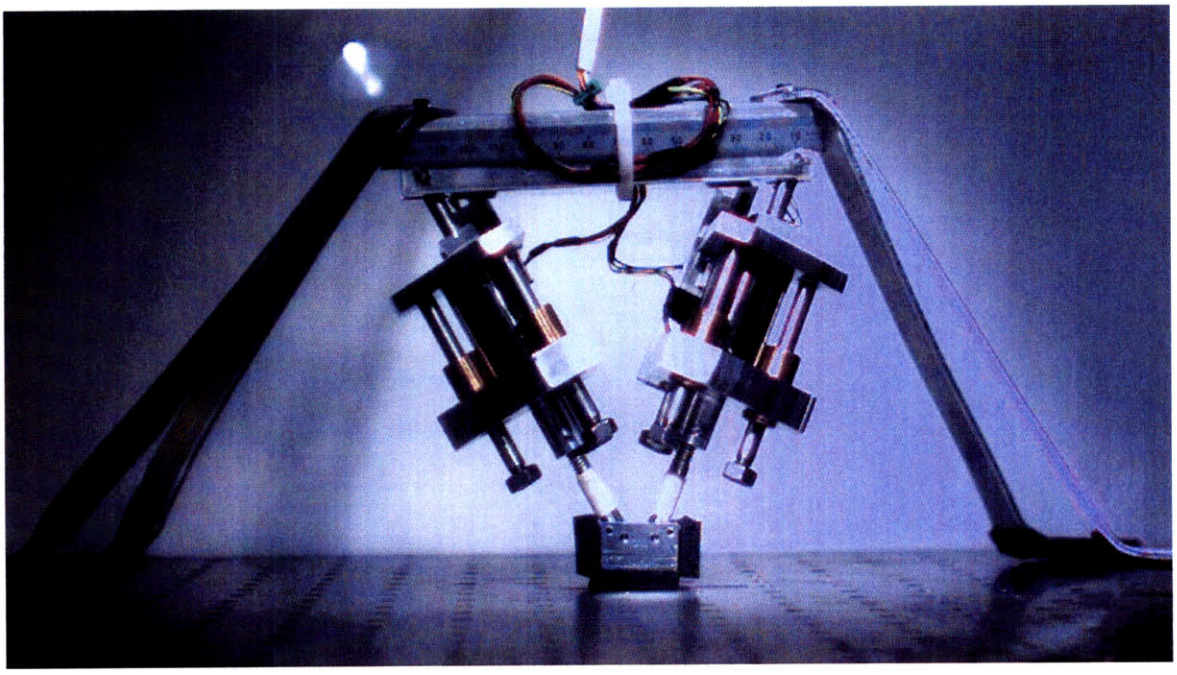

Figure 35. High speed camera image of jump – finish. The robot has landed and is now at rest. The motors are fully retracted, and the robot is ready for another jump.

6.0 Conclusions and Recommendations

Our work supports the feasibility of a VCM-driven mobile robot. The robot was able to jump three times higher than its actuator stroke. If a larger voice coil were used, the robot would likely be able to jump over many types of obstacles encountered off-road. The major challenge would be in powering such a robot, as it would require very large bursts of energy. Perhaps a large capacitor array could provide sufficient power.

Future work on this project would begin with determining the maximum jump height that the motors can withstand. This would require a larger power supply, probably at least 100 V, and a stronger power MOSFET. Working to reduce the weight of the robot would also help increase the jump height.

The next step in the project could expand the robot to provide another degree of freedom in the leg. A 3 DOF leg could be made by simply adding another VCM in parallel with the current two motors. Unfortunately, this would likely require an extensive redesign.

This idea could also be applied to make a robot capable of standing on its own. A robot with three legs, each of which has 3 DOF, could be completely self-supporting. It could likely run very quickly, as each of the legs would be able to move at maybe 100 Hz. The legs could operate independently for fast running, or they could operate in unison to achieve a higher jump to overcome an obstacle.

With today's advances in magnet and energy storage technologies, a VCM-powered robot could be very successful in the near future. The high speed and efficiency of VCMs could allow them to outperform mobile robots currently on the market.

References

1. Basak, Amitava. 1996. Permanent-Magnet DC Linear Motors. Oxford University Press, USA.

2. Raibert, M. H., Brown, H. B., Jr., Chepponis, M. 1984. Experiments in balance with a 3D one-legged hopping machine. *International J. Robotics Research\/* 3:75--92.

3. MIT Leg Laboratory. http://www.ai.mit.edu/projects/leglab/robots/3D_hopper/3D_hopper.html

4. Squire, J. 1981. The Structural Basis of Muscular Contraction. New York: Plenum Press.

5. Davies, D. V. (Ed.). 1962. Grays Anatomy. (32 ed.). London, WI: Longmans, Green, and Co., Ltd.

6. V. Gough and S. Whitehall, "Universal tyre test machine," in *Proc.FISITA 9th Int. Technical Congress*, May 1962, pp. 117–137.

7. Gough V. E. Contribution to discussion of papers on research in automobile stability, control, and tyre performance, 1956-1957. Proc. Auto Div. Inst. Mech. Eng.

8. Collins, C.L. University of California, Irvine. http://synthetica.eng.uci.edu/~curtis/project2.html

9. Parallel Robotic Systems Corporation. www.prsco.com

10. Takanishi Laboratory, Multi-purpose Biped Locomotor. http://www.takanishi.mech.waseda.ac.jp/top/research/parallel/right.html

11. Merlet, J.-P. Parallel robots. Dordrecht: Springer, 2006.

12. Condon, E. U. and Odishaw H. 1967. *Handbook of Physics* (2nd ed.). New York: McGraw-Hill Book Company.

13. Taberner, A. Ball, N. Hogan, C. Hunter, I. A Portable Needle-Free Jet Injector Based on a Custom High Power-density Voice-coil Actuator. Proc. 2 8'h IEEE Conference, Engineering in Medicine and Biology Society, 5001-5004, 2006

14. Moticont a Motion Company – 6901 Woodley Avenue, Van Nuys, CA 91406. www.moticont.com

15. IXYS Power. www.ixyspower.com

16. Agilent Technologies, Inc. 5310 Stevens Creek Blvd., Santa Clara, CA 95051. www.agilent.com

17. National Instruments Corporation. 11500 N Mopac Expwy., Austin, TX 78759. www.ni.com

18. Vision Research, Inc. 100 Dey Road, Wayne, NJ 07470. www.visionresearch.com

Appendix 1

MATLAB script to determine foot range of motion and force as a function of leg-to-base length ratio

```
la=0.2;         %base length [m]
qb_max=0.0151; % maximum displacement of motor on leg b
qc_max=q1_max; % maximum displacement of motor on leg c
Fb=1;           % actuation force of motor on leg b
Fc=1;           % actuation force of motor on leg c

% determine range and force for different leg length ratios
k=0;
for lb=.6*la:.001:1.5*la
    lc=lb;
    j=0;
    for qb=0:.0005:qb_max;
        for qc=0:.0005:qc_max;
        theta_c=acos((la^2+(lb+qb).^2-(lc+qc).^2)./(2*la*(lb+qb)));
        theta_b=acos((la^2+(lc+qc).^2-(lb+qb).^2)./(2*la*(lc+qc)));
        x3=(lb+qb).*cos(theta_c);
        y3=-(lb+qb).*sin(theta_c);
        j=j+1;
        pos(j,1)=x3;
        pos(j,2)=y3;
        q_vec(j,1)=qb;
        q_vec(j,2)=qc;

        F(j,1:2)=[Fb*cos(theta_c)+Fc*cos(theta_b)
                  Fb*sin(theta_c)+Fc*sin(theta_b)];
        end
    end
    x_range = range(pos(:,1));
    y_range = range(pos(:,2));

    k=k+1;
    F_mean(k,1:2)=[mean(F(:,1)) mean(F(:,2))];
    range_vec(k,1:2)=[range(pos(:,1)) range(pos(:,2))];
    ratio(k)=lb/la;
end
% Plot of X Range and Y range
figure(1)
m=plot(ratio,range_vec(:,1)*1000,'k-',ratio, range_vec(:,2)*1000,'b:');
title('Range of motion of foot as function of leg length ratio')
ylabel('Range of Motion (mm)')
xlabel('Ratio of Leg to Body Length')
legend('Horizontal','Vertical')
%Plot of mean force vs. ratio
figure(2)
h=plot(ratio,F_mean(:,1),'k-',ratio,F_mean(:,2),'b:');
legend('Horizontal', 'Vertical')
title('Mean Force as function of leg length ratio')
xlabel('Ratio of Leg to Body length')
ylabel('Ratio of Movement to Actuation Force')
```